Proceedings World Geothermal Congress 2015
Melbourne, Australia, 19-25 April 2015

Progress in Understanding the Physics of Large Induced Seismicity at Basel, Switzerland

Yusuke Mukuhira, Hiroshi Asanuma and Markus Häring

Institute of Fluid Science, Tohoku University, 2-1-1 Katahira, Aoba-ku, Sendai 980-8577, Japan

mukuhira@geo.ifs.tohoku.ac.jp

Keywords: HDR/EGS, microseismicity, stimulation, magnitude, large events, Basel

ABSTRACT

Several seismic events with moment magnitude larger than 2.0 occurred during and after a hydraulic stimulation in Engineerd Geothermal System (EGS) project at Basel, Switerland. This large event caused damage to buildings, which led to the cancellation of the EGS project. The authors have investigated the physics of the large events in order to learn from this experience, mitigate seismic hazard risk, and control the magnitude of the seismic events during stimulation in the future. The fundamental characteristics that were used to distinguish the large events from the small ones were hypocenter location, occurrence time, time series occurrence, waveform similarity to the other events, fault plane solutions, seismic source parameters, and stress drop. These characteristics revealed that the large events occurred in the deep part of the reservoir; events from the shallow part of the reservoir had different occurrence times and different waveforms. Based on the fundamental characteristics of the large events, we estimated an increase in pore pressure, diffusion pressure, and static stress change caused by the preceding events, which are possible trigger mechanisms of the shear slip. We investigated the relationship between these parameters and the occurrence of the large events. We found that an increase in pore pressure, which has been recognized as the main trigger mechanism of stimulation, cannot fully explain the occurrence of the large events, even though pore pressure is still the most reasonable trigger mechanism, considering a small change in diffusion pressure and static-stress change. These results indicated the dynamic behavior of the pore pressure and the thermal effects on the stress should be investigated further. Investigation of the control factor of the event magnitude has been in progress. We found that large events were likely to occur from the fault plane, where large shear stress exists. Hence, we concluded that the shear stress is one of the trigger mechanisms of the large events; however, the existence of other contributing factors to event magnitude are also suggested.

1. INTRODUCTION

Hydraulic stimulation is a key technology for enhancing the permeability of formations or to improve the system productivity of Enhanced/Engineered Geothermal System (EGS) projects, and has been used in many EGS projects to attempt to create economic reservoirs. This technology is similar to “fracking” for the extraction of unconventional resources such as shale gas and oil. Such fluid injection can induce shear slip on existing fractures or can initiate fractures, and the release of acoustic energy is often observed as induced seismicity, and is seen as the evidence of these phenomena.

Because the magnitude of observed induced seismicity is typically less than 1.0, it is seldom perceived by humans. However, one of the problems associated with hydraulic stimulation is the occurrence of the seismic events of sufficient magnitude to be felt on the surface (Majer et al., 2007; Suckale, 2009). These large-magnitude events can cause seismic hazards, and their impact on the reservoir is not well understood. Therefore, regulations or protocols based on scientific knowledge have been demanded by industry and by the public. A better understanding the physics of the large events, and the development of methods to control the magnitude of seismic events, is necessary to mitigate the risk. To achieve this understanding, several studies have been carried out (e.g., Shapiro et al., 2010; Evans et al., 2013; Ellsworth, 2013).

However, poor large-event data and other geophysical data of poor quality make it challenging to the study of large-magnitude events. In most geothermal development, even the waveforms of large events were not recorded, or the waveforms were saturated. This is because the dynamic range of monitoring systems was limited, or microseismic monitoring was not operating in the post-stimulation phase. These data problems related to analysis of large events made it difficult to even determine the hypocenter of the events, or to estimate seismic source parameters.

This study solved these problems by using a high quality dataset and other geophysical information from the Basel, Switzerland, EGS project. This dataset gave us the opportunity to investigate the physics of the large events directly by analyzing real datasets of good quality. The authors analyzed seismic events observed during and after stimulation in the EGS project at Basel in 2006 (Asanuma et al., 2008). In this paper, the result of fundamental analysis of the large events and the characteristics of the large events is documented. The details were summarized in Mukuhira et al. (2013). Subsequently, we describe in more detail the physics of the trigger mechanism and the factors that control magnitude.

2. OUTLINE OF THE DATASET USED IN THIS STUDY

Geothermal Explorers Ltd. (GEL) drilled the Basel-1 injection well in an urban area to a depth of 5 km into crystalline basement rock (GEL is now known as Geo Explorers Ltd.). Hydraulic stimulation was then conducted in the lowermost section of Basel-1 in December 2006. A total of 11,500 m^3 of fluid was injected in 6 days. The maximum wellhead pressure was about 30 MPa at a flow rate of 50 L/s (Häring et al., 2008). The injected water stimulated some existing natural fractures in the open-hole section. The well designed seismic monitoring system consisted of 6 permanent seismometers in boreholes and 1 temporary seismometer in the injection well. The signals recorded in the initial period of the stimulation in a temporary station were used to improve the velocity model and the station correction values for hypocenter determination. Analog to digital conversion at the wellhead with 1 kHz sampling frequency resulted in acquisition of a high signal to noise ratio and clear waveforms of even large-magnitude events.

Microseismic activity was continuously monitored for a half year. By February, 2007, more than 13,000 seismic events were detected. Using a conventional absolute mapping technique, Asanuma et al. (2007) determined the hypocenter locations of about 2,900 seismic events. The hypocenter distribution of the seismic events delineated a sub-vertical planar seismic cloud with a strike of about NNW-SSE. This was consistent with the regional stress state at Basel. Asanuma et al. (2008) relocated hypocenter positions using the multiplet analysis technique (Moriya et al., 2003) and the double difference method (Waldhause and Ellsworth, 2000). Their investigation showed that the stimulated reservoir at Basel consisted of a sub-vertical linear or planar structure. Their works also showed that these microscopic seismic structures were oriented ±30° from N144°E ± 14°, which is the orientation of the maximum horizontal stress estimated by Valley and Evans (2006).

3. THE PHYSICS BEHIND THE LARGE EVENTS AT BASEL

The process of achieving an understanding of the large events at Basel consisted of three stages. The first stage was an investigation of the characteristics of large events to discover event details. The second stage was the identification of the parameter and its behavior in triggering large-event shear failures. Generally, during fluid stimulation, injected fluid decreases the effective normal stress, at which point shear slip occurs. Our study accepted this principle, and that the pore pressure can be the major trigger mechanism of large events. However, the occurrence of large events is an unexpected phenomenon that is beyond our present understanding of induced seismicity. Therefore, the contribution of other parameters to triggering the shear slip – in the Coulomb failure criterion, stress change, or friction coefficient – were also investigated. The third stage was the study of the control factor of event magnitude. Based on the Coulomb failure criterion, the contribution to the event magnitude of pore pressure, stress state, and friction coefficient were investigated. The conditions when shear failure propagated in the wide part of the fault were constrained.

3.1 Characteristics of the large events

In this study, we focused on the seismic events with moment magnitude (Mw) > 2.0, because events with Mw > 2.0 were often felt by the local population. Magnitude time history is shown in Figure 1 with the hydraulic record. The large events occurred during and after the stimulation. Several large events occurred within a day of the stimulation. Some of these large events (including the largest, at Mw 3.51) had hypocenters in the deep part of the seismic cloud. This is shown in Figure 2. Others occurred in the middle part of the seismic cloud. Although wellhead pressure had returned, hydrostatic and seismic activity became low within several days of the stimulation. Nonetheless, several large events occurred as late as one or two months after stimulation.

The hypocenters of the large events in the post stimulation phase were in the middle to shallow part of the seismic cloud. Figure 2 shows the location of the two largest events in the post stimulation phase. These were shallow events located outside of the seismic cloud. There is a possibility that these two shallow events actually occurred within the seismic cloud, because spatial errors in their hypocenter determination were about 100 m, much larger than the spatial errors of smaller events and other large events.

The first large event from the deep part of the seismic cloud occurred on December 8, 2006, when the well-head pressure was 30 MPa. Before the occurrence of the first deep large events, the seismic cloud had extended to the deep part of the reservoir. Subsequently, several large events, including the largest, followed, even when hydraulic stimulation stopped. For two days after the shut-in, the seismic cloud extended mainly to the upper part of the reservoir. Due to the complicated fracture system in the deep part of the reservoir, it was quite difficult to identify the foreshocks and aftershocks of the large events. A clear extension of the seismic cloud after the occurrence of the reservoir has not been observed, though this was observed in other EGS fields such as Cooper Basin, Australia (Asanuma et al., 2005).

Fault plane solutions (FPSs) for some seismic events were estimated by Deichmann et al. (2009), using the Swiss Seismological Service (SED)/ETH monitoring network for natural earthquakes. FPSs of 28 larger events were precisely determined, most showing a strike slip type of focal mechanism. Our study was constrained to actual failure planes from a couple of nodal planes, considering the shear/effective stress working on each nodal plane, based on the orientation of stress state (Valley and Evans, 2006) and stress magnitude information (Häring et al., 2008). The result of identifying the failure planes of 28 seismic events is summarized in Figure 3 (a). The large events occurred mainly along two types of the fault planes. Many of the large events occurred along a fault plane with a N-S strike. A few large events from the deep part of the reservoir had an FPS of WNW-ESE azimuth. The fault planes of these deep large events overlapped spatially. Figures 3 (b) and Figure 3 (c) show, respectively, the rose diagram for the azimuths of all multiplet events and the rose diagram for the azimuths of microscopic seismic structures. It is shown that the large events occurred from a particular fault plane despite the fact that smaller events occurred from variously oriented fault planes.

The seismic source parameters were inferred from S-wave spectra recorded at Riehen 2 Station, and the stress drops at the shearslip of the seismic events were calculated. Seismic moment and rupture area shows linear correlation in logarithmic scale, suggesting that the "constant stress drop scaling law" can be applied to the shear slip of a series of the seismic events at Basel.

The fundamental characteristics of the large events revealed by our previous study (Mukuhira et al., 2013) were summarized in Table 1. This also includes other characteristics, such as waveform similarity, which were not described in this paper (please see Mukuhira et al., 2013). The large events that occurred in the deep and shallow parts of the reservoir showed different characteristics in their occurrence time, waveform similarity, and FPSs. The orientations of the azimuth of the strike slip fault planes of the large events were distributed asymmetrically to the orientation of the maximum horizontal stress. This observation showed a trend of the fault plane where the large events could have originated. The estimated stress drop showed the "constant stress drop scaling law" among seismic events, including the large event, suggesting that the shear slip, which was the origin of the large events, is not a peculiar phenomenon such as shear slip with extremely high stress drop.

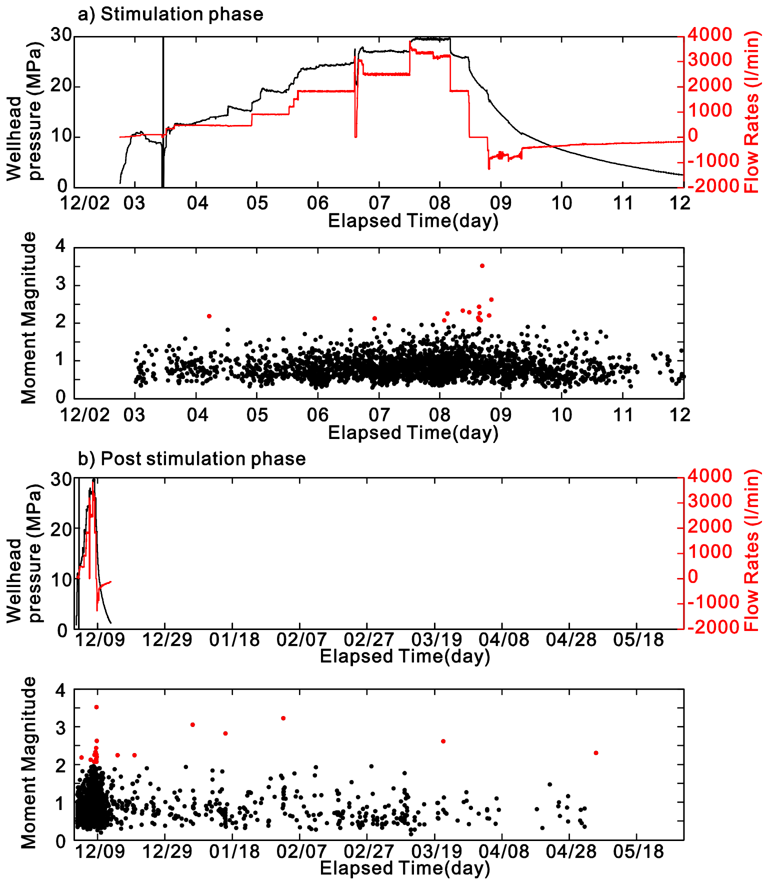

Figure 1: The time history of moment magnitude of the seismic events with the hydraulic record. a) During and just after the stimulation, b) Post stimulation phase; a half year after the stimulation.

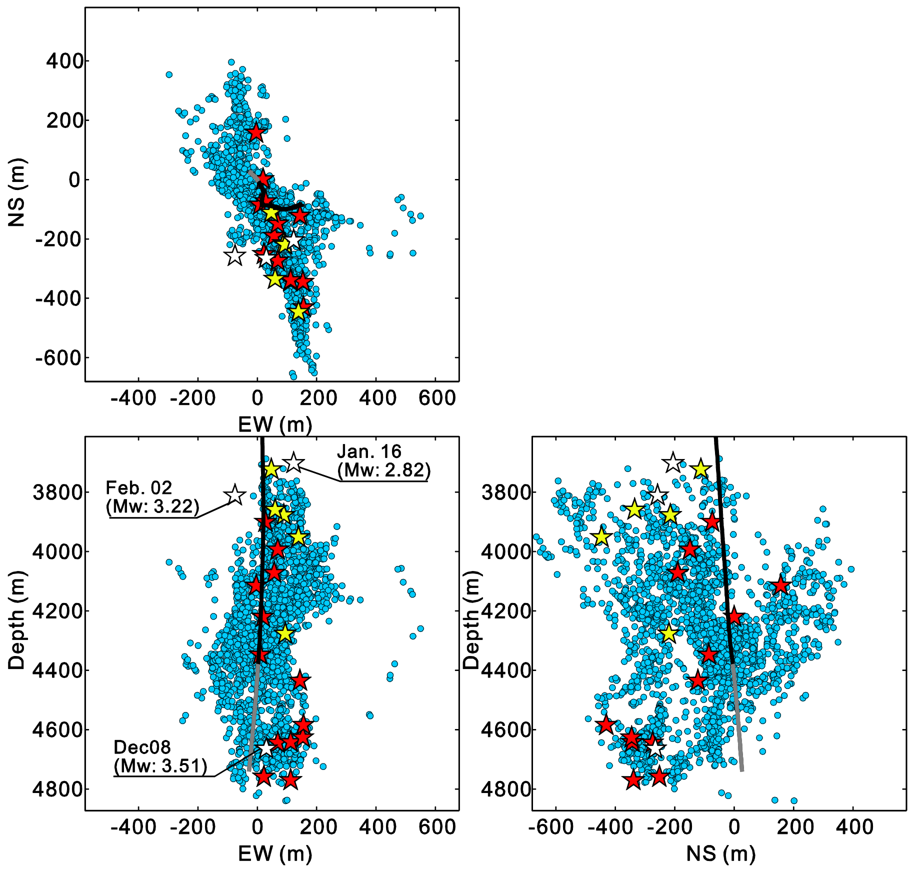

Figure 2: The hypocenter location of microseismic events (blue circles), the largest event, shallow large events (white stars), and other large events (by 12 December: red star, after 12 December: yellow star) determined by DD method. The sub-vertical line in lower diagram shows injection well trajectory; the gray parts indicate the open-hole section.

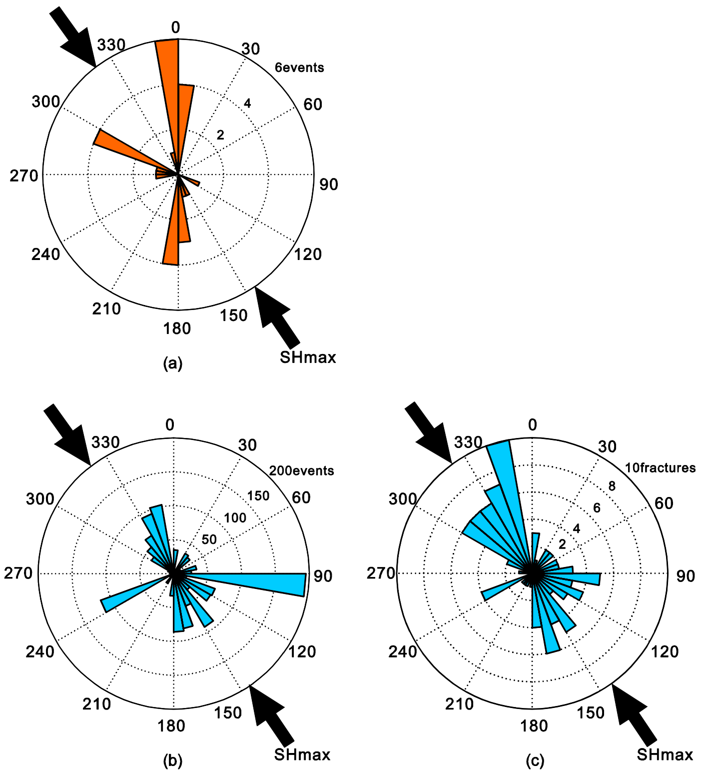

Figure 3: (a) The lower hemisphere projection of pole distribution of identified fault planes for the 28 largest events. (b) The rose diagram of azimuths for all multiplet events. The dispersion of orientations of azimuth for all multiplet events is shown. (c) The rose diagram of azimuths for multiplet seismic structures derived from multiplet analysis. This figure indicates the distribution of the azimuths of microscopic seismic structure. Arrows show the orientation of regional horizontal maximum stress.

Table 1 Characteristics of the large events that occurred from the deep and shallow parts of the seismic cloud.

	Deep large event (4600 m~ deeper)	Shallow large event (~3900 m shallower)
Occurrence time	- Some large events occurred during the stimulation - The largest event and several large events occurred within a day of the shut-in	- Mw 2.82 occurred one month after the shut-in - Mw 3.22 occurred two months after the shut-in
Hypocenter location	- Occurred from inside the seismic cloud - Occurred from high seismic activity area in the final stage of the stimulation	- Occurred outside of the seismic cloud
Timeseries occurrence	- Seismic cloud extended to the deep part of the reservoir, then large events began to occur - Following large events, occurred from already stimulated area or the edge of the seismic cloud - No clear extension or aftershock was observed	- Occurred one or two months after the shut-in - Seismic activity has not declined, even one month after the stimulation - No foreshock was observed before the occurrence of the shallow large events
Similarity in waveform	- High waveform similarity to the neighboring events - Similarity decreases with the distance - High waveform similarity between the large events	- Low waveform similarity to most of the seismic events
FPSs	- All FPSs of the large events were strike slip type - The large events occurred mainly from two types of fault planes, striking WNW-ESE and N-S - Many of the large events occurred from N-S strike fault plane - Only three large events (including the largest) occurred from fault plane of WNW-ESE strike	
	- Deep large events and the largest events have FPS to that of WNW-ESE strike - Some of the large events occurred from a part of the fault plane of the largest event	- N-S strikes - Spatially separated from the main seismic cloud
Source parameters	- Source radius of the large events was about 50~180 m	
		- Source radius of the shallow large events were relatively large compared to deep large events with similar magnitude
Stress drop	- Most of the stress drop of seismic events was less than 1 MPa - The stress drop of the large events was 1~3 MPa - "Constant stress drop scaling law" exists between seismic moment and fault area	

3.2 Trigger mechanism of the shear slip of the large events

The shear slip of the existing fracture is described by Coulomb failure criterion, where three parameters—pore pressure, shear/normal stress working on the fault plane, and the friction coefficient—can trigger shear failures. The pore pressure increase, and static stress changes caused by shear slip of the preceding seismic events, were estimated and discussed the relationship to the occurrence of the large events.

3.2.1 Pore Pressure

It is well understood that injected pore pressure is a principal trigger of shear slip on existing fractures (Brune and Thatcher, 2002); this is the principle of hydraulic stimulation. Critical pore pressure for shear slip can be estimated from the Coulomb failure criterion, using the information of the stress state around the reservoir, the orientation of the fault planes, and estimates of friction coefficient. The orientation of maximum horizontal stress has been estimated by Valley and Evans (2009) and stress magnitude has been constrained by Häring et al. (2008). Based on this information, critical pore pressure was computed for 27 seismic events that Deichmann et al. (2009) used to estimate their FPSs. Critical pore pressure for multiplet events was similarly estimated, using the orientation of multiplet seismic structure from their hypocenter distribution (Asanuma et al., 2008).

The seismic events are shown with estimates of critical pore pressure in Figure 4. A time series of the critical pore pressure for deep large events and their neighboring small events was selected from the most seismically active area. These are also shown in Figure 4. This analysis revealed that the large events occurred under moderate critical pore pressure. There was no significant increase in pore pressure prior to the occurrence of the largest event in the seismically active region. In the given area, at least one day before the largest events, pore pressure had increased to larger than the critical pore pressure of the largest event. These observations suggest that the increase in pore pressure should still be considered as the main trigger mechanism. However, the increase of pore pressure cannot explain fully the evolution of the shear slip of the large events. Figure 5 shows the 1-D spatio temporal distribution of the pore pressure estimated from the diffusion model proposed by Dinske et al. (2010), where the pore pressure propagation was described by the diffusion process. Here, a linear approximate function of the well head pressure was used as input function, and diffusivity was estimated from our hypocenter distribution to be 0.0031 m^2/s. The diffusion model simulated the MPa order of increase in diffusion pressure only near the field of the feed point. The diffusion pressure decreased exponentially with the distance from the feed point. As a whole, the pore pressure change calculated with the diffusion model was much smaller than the pore pressure change estimated with Coulomb failure criterion. This is because the behavior of pressure propagation was modeled as a diffusion phenomenon in a porous media in a diffusion model. Meanwhile, diffusion pressure had been disturbed in the far field even after two months of stimulation, although the magnitude of the change was quite small.

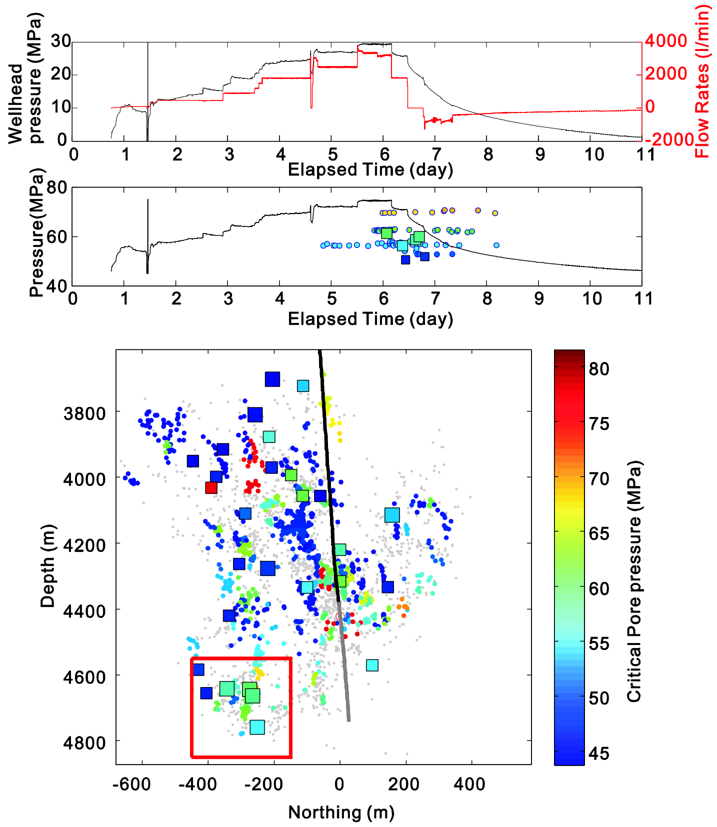

Figure 4: Time series of hydraulic injection records (upper). Critical pore pressure for a series of microseismic events (middle) from the zone of high microseismic activities indicated by the red square in the lower panel. Color coding for the event pore pressure is the same as in the lower panel. The black line on the middle panel is downhole pressure estimated from wellhead pressure. The lower panel shows the spatial distribution of critical pore pressure in the N–S vertical cross section. The black subvertical line is the trace of the injection well; the gray part of the line indicates the open-hole section. Solid squares show hypocenter locations and critical pore pressure derived from FPS, and especially large events are shown with large squares. Circles show those derived for multiplet planes. The color scale represents the magnitude of critical pore pressure.

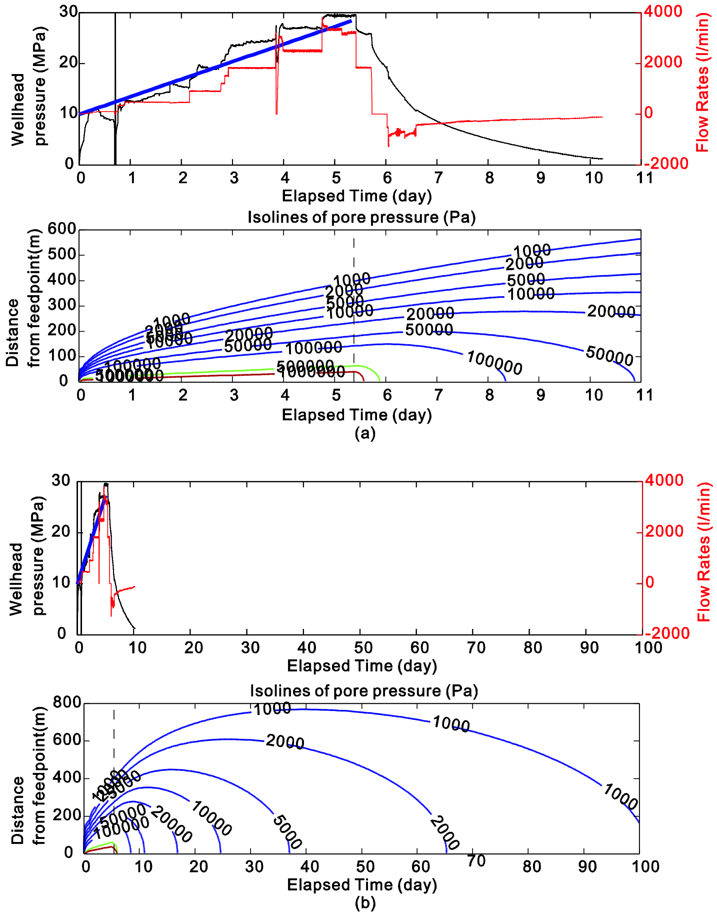

Figure 5: Hydraulic record and input function for the diffusion model, with blue line in upper panel in (a) stimulation phase and (b) after 100 days from the start of the stimulation. The 1-D pore pressure distribution is shown with isolines in lower panels.

3.2.2 Stress Change

Theoretically, stress state changes on the fault plane can trigger the shear slip of an existing fracture. However, several phenomena, such as volumetric strain caused by massive fluid injection or thermal strain caused by temperature difference between hot rock mass and cold injected water, can cause stress redistribution. We focused on the static stress change caused by preceding events and investigated the occurrence of the large events in this study. Coulomb3 software (Lin and Stein, 2004; Toda et al., 2005) enables users to calculate the static stress change from information on the orientation of the fault planes and seismic source parameters (magnitude, fault area, and slip displacement). We used the FPSs of the 28 relatively large events as source faults, which brought stress change on the target fault because their FPSs were more reliable than those estimated by multiplet analysis, and larger events dominantly brought stress redistribution. We estimated seismic source parameters in our studies (e.g. Mukuhira et al., 2013), which were also used for input in the Coulomb 3 software.

Figure 6 shows a time series of the average Coulomb stress change on the fault plane of the largest event (middle panel). Significant increase in Coulomb stress change prior to the occurrence of the largest event was not observed. Coulomb stress on the given fault decreased, suggesting the fault became stable. Detailed stress changes were calculated for each 16 elements of the divided fault plane of the large event, as we showed in Figure 6 (lower panel). The other colored faults indicate the fault planes of seismic events with relatively large magnitude, of which SED estimated FPSs (Deichmann et al., 2009). These events occurred before the largest events, and they were used as source faults to cause static stress change on the fault plane of the largest event. Calculation results showed that some part of the fault plane of the largest event had 1 bar (0.1 MPa) of positive Coulomb stress change, which drives the fault to the failure. Meanwhile, on the other part of the given fault plane, negative stress change was also observed. The typical change in Coulomb stress was less than 10 bar (1.0 MPa), at maximum in this case. This is also a much smaller change; more like diffusion pressure than pore pressure from Coulomb failure criterion. Therefore, the shear slip of the microseismic events induced by the hydraulic stimulation have too little effect to trigger the shear slip on the other fault planes, unless the events have a large magnitude or the target fault is located very close to the source fault.

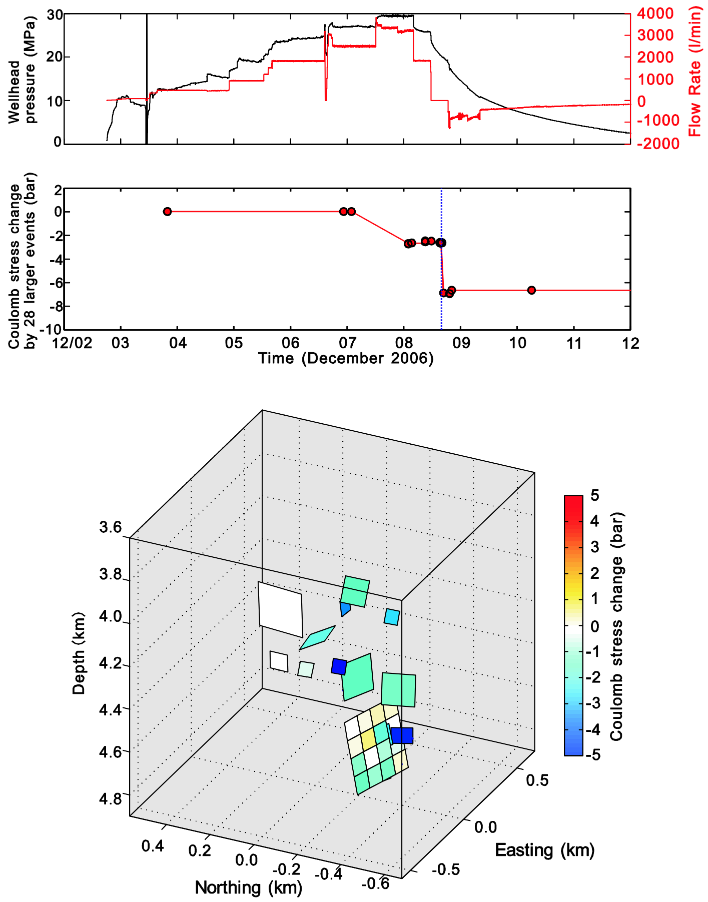

Figure 6: Pumping records (top) and time series of average Coulomb stress changes on the fault plane on which the largest event occurred (middle). The blue broken line in the middle diagram is the occurrence time of the largest events. Detailed Coulomb stress changes on the fault plane (divided into 16 patches) where the largest induced event occurred.

3.3 Control factor of event magnitude

According to seismology theory, the event magnitude or seismic moment is defined as a product of the fault area and shear displacement. On the other hand, the shear slip of the existing fracture was described by the Coulomb failure criterion. To specify the controlling factor of the event magnitude, the relationship of the parameters in the Coulomb failure criterion to the magnitude or fault area/slip displacement should be investigated. Using estimates of pore pressure and the stress state on the fault plane in the process of the investigation of the trigger mechanism, these parameters were compared with the event magnitude. Figure 7 shows the cross plot between the moment magnitude and critical pore pressure for shear slip estimated from Coulomb failure criterion. Information on the FPSs of 118 seismic events, which were also estimated by SED (Terakawa et al., 2012), were used to increase the plots. The reliability of the FPSs was comparable to 28 well constrained FPSs (Deichmann et al., 2009). Figure 7 shows there was clear negative proportional correlation between the moment magnitude and the increase in pore pressure, when the plot of the largest event was neglected. At most, it is probable that the large events were likely to occur under a low increase in pore pressure. The comparison between the shear/normal stress working on the fault planes and the event magnitude are shown in Figure 8. It is clearly shown that the large events were likely to occur from the fault planes with the large shear stress. Meanwhile, no clear correlation existed between the normal stress and moment magnitude.

4. DISCUSSION

From the fundamental characteristics revealed by our series of studies, the large events that occurred at Basel had different features, depending on their occurrence time and locations. The largest event (with Mw 3.51) and several other large events occurred during and just after the shut-in from the deep part of the seismic cloud. As deep large events showed high waveform similarity to the neighboring events, their hypocenters were likely to locate within the seismic cloud. At the Cooper Basin hot fractured rock (HFR) field, it has been reported that the large events occurred at the edge of the seismic cloud and, following the sequence of the seismic events, showed the clear extension of the reservoir (Asanuma et al., 2005). However, the deep large events at Basel did not occur at the edge of the seismic cloud at that time, and no clear extension or after shock were observed in the time series distribution of the seismic events. Therefore, large events at Basel cannot be explained by the simple asperity model that can be applied to the large events at Cooper Basin. Moreover, the largest events, and two other large events, were likely to occur along the common fault with WNW-ESE strikes, suggesting that shear failure occurred at different scales on the same fault plane at least three times.

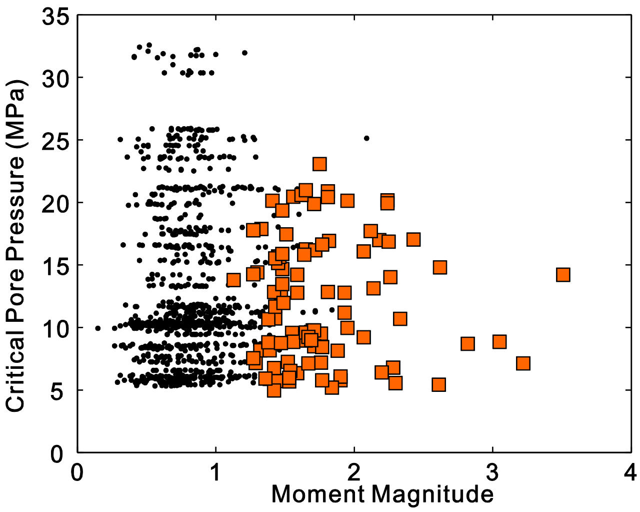

Figure 7: Correlation between moment magnitude and delta pore pressure. Squares show critical pore pressures derived from FPSs for large events and circles show those derived from multiplet planes.

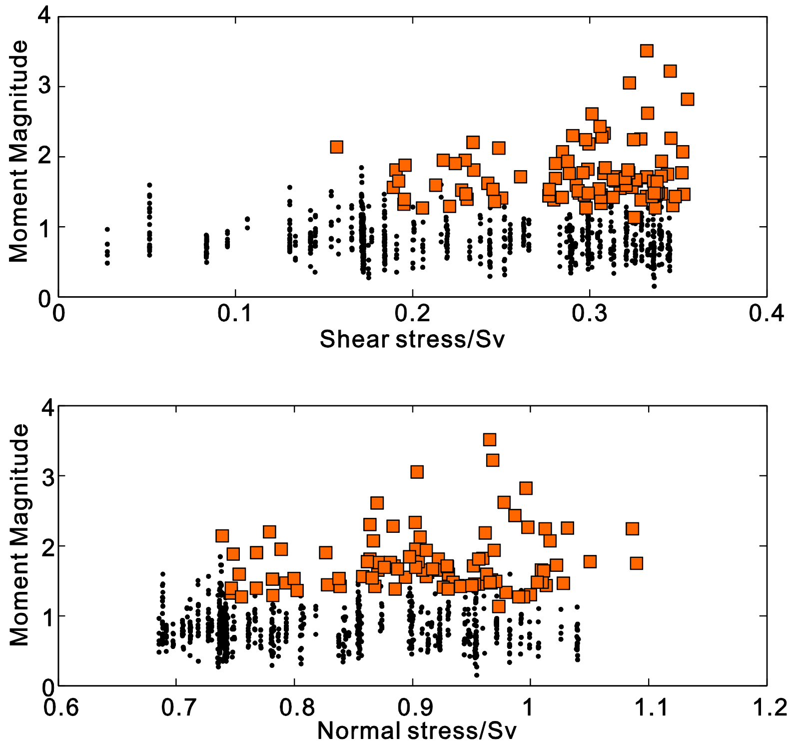

Figure 8: The relationship between normalized shear stress and moment magnitude of the seismic events at Basel. Squares correlate the events of which FPSs were estimated by SED and dots correlate the events of which FPSs were estimated for multiplet events.

Two large events that occurred one or two months after the hydraulic stimulation had hypocenters at a shallow depth and outside of the seismic cloud. Because of the large uncertainty in the hypocenter determination, there was some possibility the events actually occurred within the seismic cloud. The low waveform similarity to other events suggests the transfer function of these large events differs from the other events, and the shallow large events were likely to occur outside of the seismic cloud. The process of reaching shear failure of the shallow large events should be different from the seismic events that occurred during the stimulation, as seismic activity became quieter one or two months after the shut-in, and injected pore pressure should have decreased almost to the hydrostatic state. If the shallow large events are located outside of the reservoir, the propagation of the pressure takes a long time, suggesting it is reasonable that the large events and moderate events occurred more than month after the stimulation.

Our analysis of trigger mechanisms for the shear slip of the large events determined that, in general, large events occurred when there was a moderate increase in pore pressure, suggesting that the fault planes of the large events were close to the critical stress state at the initial state. Meanwhile, it is observed that some smaller events occurred under a small increase in the pore pressure from the area where large events subsequently followed. Therefore, it can be assumed that the large events did not occur even after the pore pressure increased enough to trigger the large events. This implies that the occurrence of the large events cannot be triggered simply by an increase in pore pressure, and that other parameters can trigger the shear slip of the large events. The inferred diffusion model suggests that the possible change of the pore pressure, even after two months of stimulation, can directly or indirectly trigger the shear slip of the large events in the post stimulation phase. However, estimated diffusion pore pressure was so small that the diffusion model cannot fully describe the occurrence of the seismic events by the pressure propagation inside and around the stimulated zone, especially during the stimulation. Pore pressure propagation surely happened after two months of stimulation, suggesting that diffusion pressure probably triggered the seismic events indirectly, in the form of thermal stress or volumetric strain. The stress change caused by the preceding events, which is the other candidate for triggering the shear slip, did not change significantly before the occurrence of the large events. In addition to this, the maximum change in Coulomb stress in this case was less than 5 bar (0.5 MPa), which is much smaller than the increase in pore pressure inferred from Coulomb failure criterion. Therefore, the stress change caused by preceding events was not the dominant trigger mechanism of the shear slip of the large events.

A controlling factor of event magnitude was also investigated, focusing the parameters in Coulomb failure criterion and the theory of seismology. A simple comparison of the moment magnitude and the critical pore pressure showed there was no positive correlation, and moreover, the large events occurred under a moderate increase in pore pressure. It was previously believed that the large events were brought about by shear slip with high stress drop from tight asperity, which could be triggered by high critical pore pressure (Charléty et al., 2007).Our observations revealed that such physical models cannot explain the phenomena of the large events at Basel. Another result supporting this interpretation is that estimations of seismic source parameters suggest that a series of the seismic dataset, including the large events, satisfy the “constant stress drop scaling law”. This means the shear slip of the large events was not interpreted as a special phenomenon where the shear slip is accompanied by a extremely high stress drop. Meanwhile, it was possible the shear stress working on the fault plane correlates with the magnitude, as shown in Figure 8. Therefore, one recent conclusion about the controlling factor of seismic events is that the large events were likely to occur along a fault plane with large shear stress. This reasonable idea has been widely accepted for mega earthquakes in subduction zones (e.g. Amelung and King, 1997). However, some seismic events with small magnitudes have occurred on fault planes with high shear stress. Therefore, other controlling factors of event magnitude should exist. Considering the fact that many large events occurred just after the shut-in, some parameters were changed by dynamic behavior of the pore pressure. This may be the key to determining the magnitude of the seismic events. Meanwhile, the fact that normal stress did not correlate with magnitude indicates that the initial state of normal stress working on the fault plane did not affect the expansion of the shear failure, and the shear stress may be dominant when the discussion is based on the idea that the scale of the shear failure is defined by the initial condition at the failure starting points. In this manner, it can be also assumed that various parameters that affect the normal stress did not affect the magnitude of the seismic events, as they cannot affect the shear stress. However, it should be noted that the propagation of the shear failure is not discussed at the point where the failure started, because the fault area, which is also a determining factor of the magnitude, should be discussed as well.

5. CONCLUSIONS

This study investigated the detailed physics behind the large events that occurred at Basel EGS project. A series of analyses of microseismic datasets and large events revealed the fundamental characteristics of the large events. These characteristics were summarized in Table 1. Some of the large events showed different characteristics, depending on their location and their occurrence time. The largest events, as well as several other large events, occurred during and after the stimulation in the deep part of the reservoir. After one or two months of the shut-in, two large events occurred at shallow depth and outside of the seismic cloud. These two types of large events had different characteristics in waveform similarity to the other events, and FPSs. Estimates of the seismic source parameter showed that the “constant stress drop scaling law” applies for the seismic events at Basel, including deep and shallow large events, suggesting the shear slip of the large events was not a peculiar phenomenon.

This study estimated some of the possible trigger mechanisms, including pore pressure, diffusion pressure, and static stress change, and discussed them in relation to the occurrence of the large events. Summarizing the new insight into the trigger of the shear slip for seismic events, the increase in pore pressure by hydraulic stimulation was still the dominant trigger mechanism for the seismic events during and just after the stimulation. However, the occurrence of large events cannot be explained by the simple theory of an increase in pore pressure. Observations that many large events occurred after the shut-in suggests the dynamic behavior of the pore pressure propagation at the shut-in should be investigated. Other possible trigger mechanisms, diffusion pressure, and static stress change caused by the preceding events did not show considerable change before the occurrence of the large events. Their change was smaller than the pore pressure estimated from the Coulomb failure criterion. However, diffusion pressure has the possibility of directly or indirectly triggering the large events after a month of the post stimulation phase, as they were still propagating at that time.

Controlling factors of the event magnitude were also investigated, based on the parameter of Coulomb failure criterion. The critical pore pressure for shear slip did not have a positive correlation with the moment magnitude. This coincided with the “constant stress drop scaling” law, suggesting that the large events were not brought by the shear slip of extremely high stress drop induced by large pore pressure. Instead, the large events at Basel occurred along the fault planes with the large shear stress. Therefore, we conclude at present that the shear stress working on the fault plane can be one of the controlling factors of the magnitude. However, there could be other factors determining the event magnitude, because smaller events also occurred along the fault planes with large shear stress.

Further study of the trigger mechanism and the controlling factor of the magnitude will be undertaken, focusing on dynamic behavior of shut-in pressure or other phenomena that can cause stress changes, such as thermal strain or volumetric strain.

ACKNOWLEDGEMENT

We thank Geo Explorers Ltd. for providing the excellent microseismic datasets and for permission to publish the results. This study was supported by the MEXT and Grant-in-Aid for JSPS Fellows (JSPS KAKENHI Grant Numbers 13J09170).

REFERENCES

Amelung, F., and King, G.: Large-scale tectonic deformation inferred from small earthquakes, *Nature*, **386**, (1997), 702–705, doi:10.1038/386702a0.

Asanuma, H., Nozaki, H., Niitsuma, H., and D. Wyborn.: Interpretation of microseismic events with larger magnitude collected at Cooper Basin, Australia, *GRC Transactions*, **29**, (2005), 87–91.

Asanuma, H., Kumano, Y., Niitsuma, H., Schanz, U., and Häring, M.: Interpretation of reservoir structure from super-resolution mapping of microseismic multiplets from stimulation at Basel, Switzerland in 2006, *GRC Transactions*, **32**, (2008), 65–70.

Brune, J., and Thatcher, W.: International Association of Seismology and Physics of Earth's Interior, Committee on Education, *International Handbook of Earthquake and Engineering Seismology*, **81A**, (2002), 569–588.

Charléty, J., Cuenot, N., Dorbath, L., Dorbath, C., Haessler, H., and Frogneux, M.: Large earthquakes during hydraulic stimulations at the geothermal site of Soultz-sous-Forêts, *International Journal of Rock Mechanics and Mining Sciences*, **44**, (2007), 11091–1105.

Deichmann, N., and Giardini, D.: Earthquakes induced by the stimulation of an enhanced geothermal system below Basel (Switzerland), *Seismological Research Letters* **80**, (2009), 78–798, doi: 10.1785/gssrl.80.5.784 8.

Dinske, C., Shapiro, S., and Häring, M.: Interpretation of microseismicity induced by time-dependent injection pressure, *SEG Expanded Abstract*, **29**, (2010), 2125, doi:10.1190/1.3513264.

Ellsworth, L.W.: Injection-Induced Earthquake, *Science*, **341**, (2013), doi: 10.1126/science.1225942.

Evans, K.F., Zappone, A., Kraft, T., Deichmann, N., and Moia, F.: A survey of the induced seismic responses to fluid injection in geothermal and CO2 reservoirs in Europe, *Geothermics*, **41**, (2012), 30–54.

Häring, M.O., Schanz, U., Ladner, F., and Dyer, B.: Characterization of the Basel-1 enhanced geothermal system, *Geothermics*, **37**, (2008), 469–495.

Lin, J., and Stein, R.S.: Stress triggering in thrust and subduction earthquakes, and stress interaction between the southern San Andreas and nearby thrust and strike-slip faults, *Journal of Geophysical Research*, **109**, (2004), B02303.

Majer, E., Baria, R., Stark, M., Oates, S., Bommer, J., Smith, B., and Asanuma, H.: Induced seismicity associated with enhanced geothermal systems, *Geothermics*, **36**, (2007), 185–222.

Moriya, H., Niitsuma, H., and Baria, R.: Multiplet-clustering analysis reveals structural details within the seismic cloud at the Soultz geothermal field, *Bulletin of the Seismological Society of America*, **93**, (2003), 1606–1620.

Mukuhira, Y., Asanuma, H., Niitsuma, H., and Häring, M.: Characteristics of large-magnitude microseismic events recorded during and after stimulation of a geothermal reservoir at Basel, Switzerland, *Geothermics*, **45**, (2013), 1–7.

Shapiro, A.S., Dinske, C., Langennbruch, C., and Wenzel, F.: Seismogenic index and magnitude probability of induced seismicity during reservoir fluid stimulations, *The Leading Edge*, **29** (3), (2010), 304–309.

Suckale, J.: Induced seismicity in hydrocarbon fields, *Advances in Geophysics*, **51**, (2009), 55–106.

Terakawa, T., Miller, S.A., and Deichmann, N.: High fluid pressure and triggered earthquakes in the enhanced geothermal system in Basel, Switzerland, *Jounal of Geophysical Research*, **117**, (2012), B07305, doi:10.1029/2011JB008980.

Toda, S., Stein, R.S., Richards-Dinger, K., and Bozkurt, S.: Forecasting the evolution of seismicity in southern California: Animations built on earthquake stress transfer, *Journal of Geophysical Research*, **110**, (2005), B05S16.

Valley, B., and Evans, K.F.: Stress orientation to 5 km depth in the basement below Basel (Switzerland) from borehole failure analysis, *Swiss Journal of Earth Science*, **102**, (2009), 467–480.

Waldhauser, F., and Ellsworth, W. L.: A double-difference earthquake location algorithm: method and application to the Northern Hayward Fault, California, *Bulletin of the Seismological Society of America*, **90**, (2000), 1353–1368.